J. Am. Chem. Soc. 1994, 116, 9257–9261

Origins of the Acidity Trends in Dimethyl Sulfide, Dimethyl Sulfoxide, and Dimethyl Sulfone

Peter Speers, Keith E. Laidig, and Andrew Streitwieser*

Contribution from the College of Chemistry, University of California, Berkeley, California 94720-1460

Received December 9, 1993. Revised Manuscript Received June 29, 1994[⊗]

Abstract: We present a theoretical study into the origin of the acidity trends in the series dimethyl sulfide (DMS), dimethyl sulfoxide (DMSO), and dimethylsulfone (DMSO$_2$). Calculations at the HF/6-31++G**//HF/6-31++G** level of theory reproduce the observed acidity trend, DMSO$_2$ > DMSO > DMS. The relative acidity is found to be an inherent property of the acid and the relative stability and geometric relaxation within the anion are unimportant. Detailed investigation of the energetics at the atomic level reveals that the origin of the relative acidities within the series is a greater destabilization of the CH_3SCH_2 fragment in the acid with increasing oxygen substitution than in the associated anion. We find no evidence in the atomic properties and the topological properties of the charge density for an appreciable delocalization of charge from the anionic carbon in the anion.

Introduction

Studies in many laboratories have provided plentiful and accurate experimental data on the acidity of various classes of compounds and the effects of substitution upon acidity, both in the gas phase[1a] and in solvents of varying polarity.[1b,c] In particular, recent studies in this laboratory have been directed toward the acidities in tetrahydrofuran of sulfur-substituted carbon acids, such as dithianes,[2] sulfides,[3] and sulfoxide and sulfones.[4] This work complements the extensive acidity studies of the Bordwell group in dimethyl sulfoxide.[1c] Apart from the inherent interest of these studies, such knowledge has become even more pertinent in recent years because of the rapid developments in synthetic methodologies utilizing regioselective carbon–carbon bond formation from sulfur-substituted carbanions.[5] Despite the accumulated body of data on this subject, the physical effects underlying the acidity of such systems remain inadequately understood. For example, the enhanced stability of α-sulfonylcarbanions has been attributed to charge delocalization by resonance of the type 1:[6] Bonding in various sulfur-substituted carbanions has also been interpreted in terms of hyperconjugation of the carbanion lone pair with appropriate orbitals to sulfur, i.e. charge transfer from n_C–σ^*(S–R) or n_C–π^*(SR_2) interactions.[7,8] Such interactions also are a charge-delocalization mechanism.

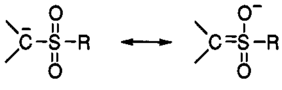
1

We present here a theoretical study of the series dimethyl sulfide (DMS), dimethyl sulfoxide (DMSO), and dimethyl sulfone (DMSO$_2$). These compounds have been studied previously by Wolfe,[9] but mainly from the standpoint of the role of d-orbital participation in the C–S bonding in the anion. Previous work[10] has shown that, although polarization functions are necessary to adequately describe the structure of dimethyl sulfone and its anion, the stabilization of the (methylsulfonyl)methyl anion is best rationalized in terms of simple Coulombic (inductive) effects. The role of d-orbitals in sulfur–oxygen bonds has recently been discussed by Patterson and Messmer.[11]

Methodology

The neutral and anionic forms of DMS and DMSO$_2$ were optimized within the constraints of C_{2v} symmetry. The lowest energy conformers of DMSO as determined by Wolfe[9] were used as starting points for the optimization of DMSO (C_s symmetry) and its anion (C_1 symmetry). All of the atomic and molecular properties were determined from HF/6-31++G** wave functions calculated at structures optimized using the same level of theory.[12] The structures were characterized by the determination of the analytical second derivatives and the frequencies were used to correct the overall deprotonation energetics for zero-point energies, which were scaled by 0.9.[13] All of the optimized structures presented were found to be true minima. The molecular calculations were performed using the GAMESS program suite.[14] The HF/6-31++G** wave function was used to determine the properties of the charge distribution and the atomic properties, using the theory of atoms in molecules as implemented within the AIMPAC suite of programs.[15] The atomic properties and energies were determined by integration of the appropriate operator over the volume (basin) of each atom.[16]

In order to relate the energy changes at both the molecular and atomic levels to physically meaningful changes of the properties of the systems without the use of arbitrarily defined characteristics, energy terms are used which are well-defined within the usual, fixed-nucleus Hamiltonian.

[⊗] Abstract published in *Advance ACS Abstracts,* August 15, 1994.

(1) (a) Pellerite, M. J.; Brauman, J. I. In *Comprehensive Carbanion Chemistry*; Buncel, E., Durst, T., Eds.; Elsevier: New York, 1980; Part A, Chapter 2. (b) Streitwieser, A., Jr.; Juaristi, E.; Nebenzahl, L. L. In ref 1a, Chapter 7. (c) Bordwell, F. G. *Acc. Chem. Res.* **1988**, *21*, 456.

(2) Xie, L.; Bors, D. A.; Streitwieser, A. *J. Org. Chem.* **1992**, *57*, 4986.

(3) White, J. J.; Xie, L.; Streitwieser, A. Results to be published.

(4) Speers, P.; Wang, P.; Streitwieser, A. Manuscript in preparation.

(5) Simpkins, N. S. *Sulphones in Organic Synthesis*; Pergamon Press: New York, 1993. *The Chemistry of Sulphones and Sulphoxides*; Patai, S., Rappoport, Z., Stirling, C., Eds.; John Wiley and Sons: New York, 1988.

(6) Carey, F. A.; Sundberg, R. J. *Advanced Organic Chemistry*, 3rd ed.; Plenum Press: New York, 1990; Part A, p 408.

(7) Wolfe, S. In *Organic Sulfur Chemistry*; Bernardi, F., Csizmadia, I. G., Mangini, A. Eds.; Elsevier: New York, 1985; Chapter 3.

(8) This interaction was invoked for related sulfonium ylides: Albright, T. A.; Burdett, J. K.; Whangbo, M.-H. *Orbital Interactions in Chemistry*; John Wiley & Sons, Inc.: New York, 1986; p 170.

(9) Wolfe, S.; Stolow, A.; LaJohn, L. A. *Tetrahedron Lett.* **1983**, 4071.

(10) Bors, D. A.; Streitwieser, A., Jr. *J. Am. Chem. Soc.* **1986**, *108*, 1397.

(11) Patterson, C. H.; Messmer, R. P. *J. Am. Chem. Soc.* **1989**, *111*, 8059. This paper also gives an extensive list of prior references.

(12) Hehre, W. J.; Ditchfield, R.; Pople, J. A. *J. Chem. Phys.* **1972**, *56*, 2257. Francl, M. M.; Pietro, W. J.; Hehre, W. J.; Binkley, J. S.; Gordon, M. S.; DeFrees, D. J.; Pople, J. A. *J. Chem. Phys.* **1982**, *77*, 3654. Hariharan, P. C.; Pople, J. A. *Theor. Chim. Acta* **1973**, *28*, 213. Frisch, M. J.; Pople, J. A.; Binkley, J. S. *J. Chem. Phys.* **1984**, *80*, 3265.

(13) Pople, J. A.; Schlegel, H. B.; Krishnan, R.; DeFrees, D. J.; Binkley, J. S.; Frisch, M. J.; Whiteside, R. A.; Hout, R. F.; Hehre, W. J. *Int. J. Quantum Chem. Symp.* **1981**, *15*, 269.

(14) GAMESS: Schmidt, M. W.; Boatz, J. A.; Baldridge, K. K.; Koseki, S.; Gordon, M. S.; Elbert, S. T.; Lam, B. *QCPE Bull.* **1987**, *7*, 115.

(15) Biegler-König, F. W.; Bader, R. F. W.; Tang, T. H. *J. Comput. Chem.* **1982**, *1*, 317.

(16) Bader, R. F. W. *Atoms in Molecules: A Quantum Theory*; Oxford University Press: New York, 1990.

0002-7863/94/1516-9257$04.50/0

We make use of the virial theorem which states that at a stationary point on a potential energy surface, the potential energy, V, given as the sum of the nuclear–electron attraction, V_{NE}, the electron–electron repulsion, V_{EE}, and the nuclear–nuclear repulsion, V_{NN}, is twice the negative of the kinetic energy of the system, T (eq 1).[17]

$$V = V_{NE} + V_{EE} + V_{NN} = -2T \tag{1}$$

Equations 2 and 3 then follow for the total energy and energy changes in deprotonation:

$$E = -{}^1/_2 V = -{}^1/_2(V_{NE} + V_{EE} + V_{NN}) \tag{2}$$

$$\Delta E = -{}^1/_2 \Delta V = -{}^1/_2(\Delta V_{NE} + \Delta V_{EE} + \Delta V_{NN}) \tag{3}$$

Since the various contributions to the potential energy are well-defined within the Hamiltonian and are related to the distribution of nuclear and electronic charges and their Coulombic interactions, the changes in the total energy of a process can be related to the changes in these distributions and the resulting changes in the interactions among them. This provides a physical picture of the changes within the system and their relation to the changes in the total energy of a system. We chose to use the SCF procedure, without the addition of electron correlation, because it correctly and adequately reproduces the energetics of deprotonation and each of the contributions to the total potential energy mentioned above is clearly defined.[18] This approach has been successfully used in a number of studies to discuss the physical underpinnings of the energetic changes within systems[19] and we apply it here at both the molecular and atomic levels to the study of deprotonation energies within the series $DMSO_x$, $x = 0, 1, 2$.

Results and Discussion

The molecular energetics and geometric parameters for DMS, DMSO, and $DMSO_2$ are listed in Tables 1 and 2, respectively. The experimental gas phase acidity ordering[20] is reproduced with our calculations; the substitution of one oxygen atom decreases the energy of deprotonation of DMS by 20 kcal mol^{-1} while the second decreases the energy by a further 11 kcal mol^{-1}. The calculated proton affinities of the anions are about 11 kcal mol^{-1} higher than the experimental results for DMS and DMSO, and 7 kcal mol^{-1} higher for $DMSO_2$. The energy changes in all three cases are dominated by a loss in nuclear–electronic attraction (V_{NE}), which outstrips a large decrease in nuclear–nuclear repulsion (V_{NN}) while the decrease in electron–electron repulsion (V_{EE}), is roughly an order of magnitude smaller. The increased acidity within the series is accompanied by a progressive increase in $|\Delta V_{NE}|$ and $|\Delta V_{NN}|$, and $|\Delta V_{EE}|$ remains nearly the same. The main geometric change associated with deprotonation is the change in the S–C bond lengths in all three systems. The anionic methylene moves much closer to sulfur with oxygen substitution ($\Delta(CH_2^-{-}S)$) bond length equals –0.046, –0.081, and –0.104 Å, respectively) upon deprotonation while the increase in the CH_3–S distance remains nearly the same ($\Delta(CH_3{-}S)$) bond length equals +0.034, +0.031, and +0.033 Å). The S–O distances in DMSO and $DMSO_2$ increase by 0.03 Å in both oxygen-substituted cases in the anion. These geometric changes do not reflect a delocalization mechanism (*vide infra*), but rather an electrostatic stabilization of the anionic methylene. This stabilization is the driving force for the increased C–S bond shortening upon deprotonation with increasing oxygen substitution. It should also be noted here that the DMSO anion adopts a conformation with a gauche arrangement of the lone pairs of oxygen and carbon, with the S–O bond staggered between the methylene C–H bonds.

Table 1. Molecular Energetics of the Neutral and Anionic Structures of Dimethyl Sulfide, Dimethyl Sulfoxide, and Dimethyl Sulfone in Comparison to Those of the Associated Anion in the Geometry of the Acid[a,b]

	DMS	Δ(DMS – DMS^{-*})	Δ(DMS^{-*} – DMS^-)	overall Δ	expl
total E	–476.746	0.664	–0.005	0.659	
V_{NE}	–1352.822	+10.939	+1.538	12.476	
V_{EE}	288.340	–1.264	–0.746	–2.010	
V_{NN}	110.990	–8.347	–0.801	–9.149	
V	–953.493	+1.327	–0.009	+1.318	
ΔE	0.0	+416.667	–3.138	+413.529	
$\Delta E + \Delta ZPE$[c]				+404.143	+393

	DMSO	Δ(DMSO – $DMSO^{-*}$)	Δ($DMSO^{-*}$ – $DMSO^-$)	overall Δ	expl
total E	–551.555	+0.645	–0.018	+0.627	
V_{NE}	–1677.572	+12.311	+0.203	+12.514	
V_{EE}	389.499	–1.1660	+0.036	–1.130	
V_{NN}	184.963	–9.85	–0.274	–10.131	
V	–1103.110	+1.289	–0.03	+1.254	
ΔE	0.0	+404.744	–11.295	+393.449	
$\Delta E + \Delta ZPE$				+384.716	+373

	$DMSO_2$	Δ($DMSO_2$ – $DMSO_2^{-*}$)	Δ($DMSO_2^{-*}$ – $DMSO_2^-$)	overall Δ	expl
total E	–626.409	+0.624	–0.013	+0.611	
V_{NE}	–2036.316	+13.738	–0.134	+13.604	
V_{EE}	507.320	–1.083	+0.23	–0.850	
V_{NN}	276.179	–11.409	–0.124	–11.533	
V	–1252.818	+1.247	–0.026	+1.221	
ΔE	0.0	+391.566	–8.158	+383.409	
$\Delta E + \Delta ZPE$				+374.286	+367

[a] The total and contributing energies are given in atomic units and have been corrected for the virial defect. The theoretical and experimental energy differences are in kcal mol^{-1} and are given relative to the neutral molecule. [b] The superscript asterisk denotes the anion at the acid geometry. [c] Energy difference corrected for zero-point energy differences (scaled by 0.9) in kcal mol^{-1}.

The properties of the electron density at the bond critical points may be used to quantitatively characterize pairwise atomic interactions (the values are listed in Table 3).[21] The properties of the critical points do not suggest appreciable movement of charge from the anionic center to the oxygen atoms. As in the geometric changes, the largest change in the bond critical points is found for the C–S interaction. The magnitude of electron density at the bond critical point for C–S in the acids increases through the series signaling an increase in the strengths of the interaction between the two atoms. The interaction increases after deprotonation with a shortening of the carbon-bonded radius as the bond length decreases. The ellipticity is a measure of dissymmetrical distribution of electronic charge at the critical point in two orthogonal planes intersecting at the bond axis, and it provides an indication of π-conjugation. There is an increase in the ellipticity of the C–S bond on deprotonation, but the principal axis of the ellipse is in the C–S–C plane; thus this is just a harbinger of the increased interaction between C and S. The S–O interaction in DMSO and $DMSO_2$ decreases after deprotonation, with slight changes in the ellipticity and small increases in the O-bonded radius. The properties of both the C–S and S–O critical points do not suggest appreciable movement of charge from the anionic center to the oxygen atoms. The interaction of carbon to the acidic proton is relatively unchanged throughout the series.

As a test of the energy observations, and to assess the amount of stabilization afforded by the relaxation of the anion, we

---

(17) Slater, J. C. *J. Chem. Phys.* **1933**, *1*, 687.

(18) For example, the MP2 energy correction does not produce a unique density matrix from which the various contributions to the total potential energy can be calculated. Use of CI-based procedures, for which the density matrix is uniquely defined, were beyond our computational abilities. For a discussion of the small differences in definitions of MP2 density matrices, see the appendix of the following: Price, S. L.; Andrews, J. S.; Murray, C. W.; Amos, R. D. *J. Am. Chem. Soc.* **1992**, *114*, 8268.

(19) Bader, R. F. W.; Cheeseman, J. R.; Laidig, K. E.; Wiberg, K. B.; Breneman, C. *J. Am. Chem. Soc.* **1990**, *112*, 6530. Laidig, K. E. *J. Phys. Chem.* **1991**, *95*, 7709.

(20) Ingemann, S.; Nibbering, N. M. M. *Can. J. Chem.* **1984**, *62*, 2273. Bartmess, J. E.; Scott, J. A.; McIver, R. T., Jr. *J. Am. Chem. Soc.* **1979**, *101*, 6047.

(21) Bader, R. F. W.; Essen, H. *J. Chem. Phys.* **1984**, *80*, 1942.

Table 2. The Geometric Parameters within Dimethyl Sulfide, Dimethyl Sulfoxide, and Dimethyl Sulfone and Their Anions[a,b]

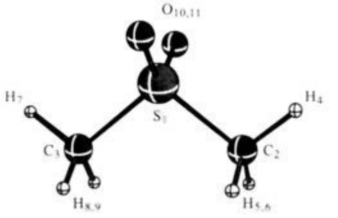

	H_4–C_2	C_2–S_1	S_1–C_3	S_1–O_{10}	O_{10}–O_{11}	H_4–C_2–S_1	H_5–C_2–S_1	C_2–S_1–C_3	C_2–S_1–O_{10}	O_{10}–S_1–O_{11}
DMS	1.082	1.808	1.808			107.44	111.07	100.10		
DMS$^-$		1.762	1.842				112.49	109.62		
DMSO	1.082	1.797	1.797	1.490		107.22	109.90	98.26	106.42	
DMSO$^-$		1.716	1.828	1.522			115.86 107.86	107.88	112.59	
DMSO$_2$	1.082	1.773	1.773	1.439	2.490	106.27	109.55	104.56	107.86	119.84
DMSO$_2^-$		1.669	1.806	1.462	2.497		113.39	112.60	110.10	117.27

[a] All bond lengths are given in angstroms and all bond angles in degrees. [b] The atoms are labeled as in the diagram.

Table 3. Bond Critical Point Properties in Dimethyl Sulfide, Dimethyl Sulfoxide, and Dimethyl Sulfone and Their Anions[a]

	$\rho(\mathbf{r})$	$\nabla^2\rho(\mathbf{r})$	ϵ	r_a	r_b
DMS					
CH_3–S	0.190	–0.385	0.103	1.629	1.787
C–H	0.291	–1.101	0.012	1.266	0.780
DMS$^-$					
CH_3–S	0.177	0.341	0.144	1.785	1.695
CH_2–S	0.197	–0.361	0.134	1.451	1.880
DMSO					
CH_3–S	0.206	–0.469	0.065	1.590	1.804
S–O	0.272	0.910	0.039	1.084	1.733
C–H	0.290	–1.098	0.006	1.275	0.772
DMSO$^-$					
CH_3–S	0.205	–0.471	0.098	1.668	1.739
CH_2–S	0.226	–0.496	0.181	1.394	1.855
S–O	0.253	0.684	0.080	1.105	1.785
DMSO$_2$					
CH_3–S	0.224	–0.555	–0.020	1.507	1.845
S–O	0.300	1.454	0.042	1.050	1.668
C–H	0.291	–1.114	0.003	1.284	0.761
DMSO$_2^-$					
CH_3–S	0.211	–0.518	0.024	1.645	1.769
CH_2–S	0.252	–0.617	0.399	1.282	1.872
S–O	0.287	1.235	0.017	1.062	1.702

[a] All values are in atomic units. The properties are determined at the (3,–1) critical point between the atoms; $\rho(\mathbf{r})$, the total charge density; $\nabla^2\rho(\mathbf{r})$, the Laplacian of the charge density; ϵ, the ellipticity; and r_a and r_b, the bonded radii.

constructed an artificial, two-step deprotonation scheme. The energetics of the anions were calculated at the geometry of the neutral molecules as a worst-case model for the unrelaxed anion (Table 1). The proton removal has the same energetic pattern as the overall deprotonation, while the relaxation of the anion shows a more even balance between $|\Delta V_{NN}|$ and $|\Delta V_{EE}|$.[19] In this series, the relaxation and the relative stability of the anion, two characteristics of a delocalization mechanism, are essentially unimportant in the increased acidity in comparison to the energy required to remove the proton. Instead, the increased acidity is associated with the characteristics of the neutral acid, the more acidic system investing more of its overall stabilization to electrostatic-like, inter-atom interaction rather than on intra-atom and shared inter-atomic interactions.

The atomic properties have been grouped into functional groups and their changes during deprotonation in Table 4.[22] The largest change in the functional group properties, as a function of oxygen substitution, is the large charge withdrawal from sulfur, the addition of each oxygen pulling 1.45 e from sulfur. The increased withdrawal of charge from sulfur results in a greater shortening of the C–S bond in the anion and the CH_2 fragment is destabilized less in the anion. The more highly charged sulfur is stabilized by both the small transfer of charge and the shortening of the C–S bond. The anionic charge of the anion is primarily localized on the methylene fragment, with a small transfer of charge to sulfur and almost no change in the population of oxygen in DMSO and DMSO$_2$. There is no significant polarization of sulfur after deprotonation, but there is a significant polarization of the methylene fragment. This would also suggest that an inter-atomic stabilization of the anionic carbon by the more positive sulfur is driving the relaxation of geometry.

The small transfer of charge to the oxygen atoms after deprotonation provides an understanding of the relatively small $|\Delta V_{EE}|$ term in the overall deprotonation. The change in V_{EE} is primarily atomic, in that most of the electron–electron repulsion occurs around individual nuclei. The small relative value of this term in comparison to the changes in V_{NE} and V_{NN} implies that the more acidic systems do not use a stabilization mechanism that involves significant electronic reorganization in the anion. This lack of charge reorganization means that the stabilization mechanism in the more acidic systems must arise from an inter-atomic or "electrostatic-like" stabilization, the attraction of the charge within each atom for the nuclei of other atoms. The formation of the anion produces forces that are minimized by moving the atoms away from each other rather than by shifting charge from atom to atom.

These data indicate that the relative acidity of DMSO$_x$ is already inherent in the acid, rather than due to any stabilization mechanisms in the anion. The relative energy changes between the acid and fixed anion suggest that this is the case, with the largest energy change associated with the separation of the proton from the acid and only a relatively small energy stabilization associated with the geometric relaxation. We also see that within the series the relative deprotonation energy is reflected in the energy change in the unrelaxed anion and the geometry relaxation does not appear to be related directly to the relative acidity. Indeed, in the limit of this observation, the magnitude of the deprotonation energy would be equal to the energy of that proton, in the absence of any charge relaxation. The calculated acidity trend in the series and the acidity differences are indeed reproduced well by the relative energies of the acidic proton, again showing that charge relaxation is relatively unimportant.

Figure 1 displays the relative energies of the CH_3SCH_2 fragment in all three acids in comparison with their corresponding anions. The neutral system is clearly seen to be more destabilized by each oxygen substitution than is the corresponding anion and this is the origin of the acidity trend. Substitution by oxygen withdraws charge from the fragment and destabilizes it, primarily destabilizing the sulfur atom. In discussing the origin of these

---

[22] A table of the full atomic properties is available in the supplementary material accompanying this paper.

Table 4. Sum of Atomic Properties for Various Fragments in the Acid and the Changes upon Deprotonation of Dimethyl Sulfide, Dimethyl Sulfoxide, and Dimethyl Sulfone[a]

	DMS	Δ	DMSO	Δ	$DMSO_2$	Δ
			CH_3SCH_2 Fragment			
$\sum N(\Omega)$	32.977	+1.023	31.528	+0.955	30.007	+0.899
$\sum E(\Omega)$	−476.108	+0.021	−475.558	−0.077	−474.628	−0.104
$\sum V_{NEO}(\Omega)$	−1133.572	−1.096	−1122.843	−2.062	−1110.709	−1.844
$\sum V_{NET}(\Omega)$	−1343.336	+2.990	−1393.403	−1.891	−1437.914	−2.765
$\sum V_{REP}(\Omega)$	391.093	+2.922	442.224	+1.735	488.554	+2.548
ΔE		+13.178		−48.318	0.000	−65.261
			CH_3 Fragment			
$\sum N(\Omega)$	9.001	+0.245	8.987	+1.104	8.905	+0.212
$\sum E(\Omega)$	−39.601	−0.070	−39.669	−0.041	−39.681	−0.068
$\sum V_{NEO}(\Omega)$	−93.239	−0.194	−93.501	−0.003	−93.496	−0.088
$\sum V_{NET}(\Omega)$	−164.208	+0.511	−178.699	+0.021	−191.762	−0.850
$\sum V_{REP}(\Omega)$	84.996	−0.653	99.340	−0.103	112.368	+0.708
ΔE		−43.926		−25.728		−42.671
			CH_2 Fragment			
$\sum N(\Omega)$	7.978	+0.657	7.982	+0.615	7.936	+0.524
$\sum E(\Omega)$	−38.964	+0.034	−39.042	+0.017	−39.069	+0.015
$\sum V_{NEO}(\Omega)$	−91.929	−0.523	−92.211	−0.544	−92.236	−0.464
$\sum V_{NET}(\pm)$	−154.728	−0.156	−167.530	−1.949	−179.842	−2.347
$\sum V_{REP}(\Omega)$	76.792	+0.226	89.427	+1.981	101.675	+2.375
ΔE		+21.335		+10.668		+9.413
			S Atom			
$\sum N(\Omega)$	15.999	+0.120	14.558	+0.213	13.160	+0.158
$\sum E(\Omega)$	−397.543	+0.056	−396.847	−0.053	−395.878	−0.051
$\sum V_{NEO}(\Omega)$	−948.404	−0.379	−937.131	−1.515	−924.977	−1.292
$\sum V_{NET}(\Omega)$	−1024.400	+2.639	−1047.174	+0.037	−1066.310	+0.432
$\sum V_{REP}(\Omega)$	229.305	−2.526	253.457	−0.143	274.511	−0.535
ΔE		+35.141		−33.258		−32.003
			O Atom			
$\sum N(\Omega)$			9.476	+0.041	9.512	+0.040
$\sum E(\Omega)$			−75.372	+0.079	−75.586	+0.053
$\sum V_{NEO}(\Omega)$			−185.325	+0.006	−185.877	−0.045
$\sum V_{NET}(\Omega)$			−272.982	+3.193	−293.216	+2.207
$\sum V_{REP}(\Omega)$			122.217	−3.035	142.006	−2.103
ΔE				+49.573		+33.258
			Acidic H Atom			
$\sum N(\Omega)$	1.023	−1.023	1.005	−1.005	0.969	−0.969
$\sum E(\Omega)$	−0.637	+0.637	−0.627	+0.627	−0.612	+0.612
$\sum V_{NEO}(\Omega)$	−1.310	+1.310	−1.290	+1.290	−1.260	+1.260
$\sum V_{NET}(\pm)$	−9.480	+9.480	−11.169	+11.169	−11.920	+11.920
$\sum V_{REP}(\Omega)$	8.204	−8.204	9.913	−9.913	10.693	10.693
ΔE		+399.724		+393.449		+384.036

[a] The sums of atomic energetics are given in atomic units and have been corrected for the virial defect. The energy differences are in kcal mol^{-1} and are given relative to the neutral molecule. $N(\Omega)$ is the population within the atomic basin, $E(\Omega)$ is the atomic contribution to the molecular energy, $V_{NEO}(\Omega)$ is the attractive energy from the charge within its own basin, $V_{NET}(\Omega)$ is the total atomic contribution to the molecular attractive energy, $V_{REP}(\Omega)$ is the atomic contribution to the molecular repulsion energy.

energetic changes, it is useful to define two quantities: $|\Delta V_{NET}(\Omega)|$, the sum of each atom's attraction between its charge and all of the nuclei within the molecule, and $|\Delta V_{NEO}(\Omega)|$, the sum of each atom's attraction between its charge and its own nucleus (the "self-stabilization"). The difference between these two quantities yields the amount of inter-atom stabilization within the fragment. This value increases from 209.8 au to 270.6 au in DMS and then to 327.2 au in DMSO and $DMSO_2$, respectively, demonstrating that the fragment depends more heavily upon inter-atom stabilization as the system becomes more acidic. However, the CH_3SCH_2 fragment is destabilized more in the acid through the series because of the great loss in self-stabilization through charge withdrawal to oxygen. The anionic fragment is less destablized as it uses the charge left after the proton is removed to relieve the stress of oxygen substitution, as can be seen by the increased values of $|\Delta V_{NEO}(\Omega)|$.

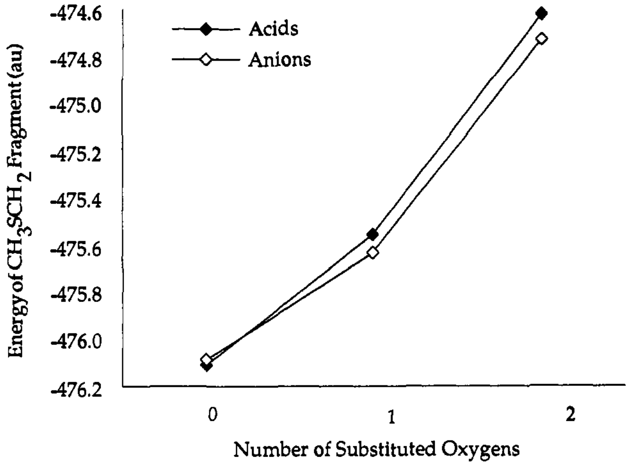

Figure 1. Total fragment energies ($\Sigma E(\Omega)$ in Table 4) in atomic units for the CH_3SCH_2 group in $DMSO_x$ as a function of oxygen substitution.

Table 5. The Electrostatic Potential at the Position of the Acidic Hydrogen Nucleus in Dimethyl Sulfide, Dimethyl Sulfoxide, and Dimethyl Sulfone[a]

	V(H)	V_E(H)	V_N(H)
DMS	−1.101	−9.443	8.342
DMSO	−1.060	−11.283	10.207
$DMSO_2$	−1.022	−12.407	11.385

[a] All values are in atomic units. V_E(H) is the contribution to the potential from the distribution of electronic charge and V_N(H) is the contribution from the nuclear framework.

Scheme 1. Energetics of Hypothetical Deprotonation Scheme[a]

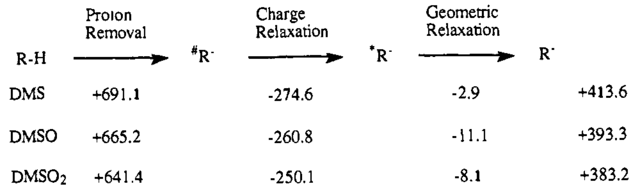

R-H	$\xrightarrow{\text{Proton Removal}}$	$^{\#}R^-$	$\xrightarrow{\text{Charge Relaxation}}$	$^{*}R^-$	$\xrightarrow{\text{Geometric Relaxation}}$	R^-
DMS	+691.1		-274.6		-2.9	+413.6
DMSO	+665.2		-260.8		-11.1	+393.3
$DMSO_2$	+641.4		-250.1		-8.1	+383.2

[a] R^- denotes the anion with both electronic charge and nuclear positions frozen, $^*R^-$ is the anion with the electronic charge relaxed but nuclei in the geometry of the acid. The rightmost number is the net deprotonation energy.

A further insight into the acidity trends in this series can be obtained from the electrostatic potential measured at the acidic hydrogen nucleus, listed in Table 5. As has been pointed out by Thomas et al.,[20] the electrostatic potential at the hydrogen nucleus multiplied by the charge of the hydrogen nucleus is the energy required to move the proton to infinity given that the rest of the charge distribution remains frozen. This provides two more steps in our hypothetical sequential deprotonation reaction: the amount of energy required to remove the proton from the fixed charge distribution and the relaxation of charge into the frozen geometry, yielding the overall deprotonation energies in Scheme 1.

This scheme provides further support for the discussion of the energetics presented above. In the more acidic systems, proton removal is more facile with increasing oxygen substitution, and the charge relaxation becomes less. The enhanced acidity is *not* due to increased stabilization of the anion or a greater charge relaxation in the substituted system but rather to a destabilization of the neutral acid, making the removal of the proton less energetically costly. The contributions to the total potential also show this trend with a more rapidly increasing nuclear contribution outstripping the increased electronic contribution leading to an overall decrease of the potential at the acidic proton.

Conclusion

These results demonstrate that the relative acidity trend in the series DMS, DMSO, and $DMSO_2$ is due to a greater destabilization of the acid with oxygen substitution than of the associated anion. The calculations adequately reproduce the experimental acidity differences and trends throughout the series. The molecular energetics reveal that the process of proton removal in all cases is dominated by a loss in nuclear–electron attraction overcoming the decrease in nuclear–nuclear repulsion, with the change in electron–electron repulsion being relatively unimportant. The relaxation of geometry following deprotonation is shown to be energetically unimportant in the overall deprotonation process, and the properties of the electron density show no appreciable transfer of charge from the anionic center to the sulfur oxygens. Resonance of the type shown in **1** is clearly unimportant. The atomic and functional group properties demonstrate that the substitution with oxygen destabilizes the CH_3SCH_2 fragment in both the neutral and anionic systems by large charge withdrawal to oxygen. Deprotonation becomes easier as the charge of the anionic center is used to stabilize the electron-poor fragment by both a small transfer of charge and electrostatic stabilization, consistent with the increasing C–S bond shortening in the anion through the series. The electrostatic energies of the acidic protons closely mirror the observed acidity trend. These results clearly demonstrate that the relative acidity is inherent in the acid and is not dependent on the geometric relaxation or delocalization of charge within the anion. Charge delocalization by hyperconjugation can make only a small contribution to the overall energetics (although such orbital interactions may be important in determining conformations). Thus, this system adds to the growing list of compounds whose enhanced acidity is already manifest in the electronic properties of the acid rather than to greater delocalization in the anion.[23,24]

Acknowledgment. This work was supported in part by NSF Grants CHE87-21134 and CHE92-21277. Some of the computations made use of the Graphics Facility of the College of Chemistry which is supported by NIH Grant S10 RR05651-01. We also thank Professor R. F. W. Bader for valuable discussions.

Supplementary Material Available: A full table of atomic properties (3 pages). This material is contained in many libraries on microfiche, immediately follows this article in the microfilm version of the journal, and can be ordered from the ACS; see any current masthead page for ordering information.

---

(23) Thomas, T. D.; Siggel, M. R. F.; Streitwieser, A. *J. Mol. Struct.* (*THEOCHEM*) **1988**, *165*, 309.

(24) Ji, D.; Thomas, T. D. *J. Phys. Chem.* **1994**, *98*, 4301. Thomas, T. D.; Siggel, M. R. *J. Am. Chem. Soc.* **1986**, *108*, 4360. Wiberg, K. B.; Laidig, K. E. *J. Am. Chem. Soc.* **1988**, *110*, 1872. Thomas, T. D. *Inorg. Chem.* **1988**, *27*, 1965. Wiberg, K. B. *Inorg. Chem.* **1988**, *27*, 3694.